COMPARATIVE INVESTIGATION BY INFRARED SPECTROSCOPY OF THE CONFORMATIONAL METAMORPHOSIS OF POLYVINYLIDENE FLUORIDE UNDER THE ACTION OF AN INFRARED LASER AND OF γ-IRRADIATION

S. R. Allayarov,[1,3] L. A. Kalinin,[2] D. A. Dixon,[3*] E. M. Tolstopyatov,[2] I. A. Frolov,[1] L. F. Ivanov,[2] P. N. Grakovich,[2] and O. N. Golodkov[1]

[1]*Institute of Problems of Chemical Physics, Russian Academy of Sciences*
Chernogolovka 142432, Russia

[2]*V. A. Belyi Metal-Polymer Research Institute, National Academy of Sciences of Belarus*
Gomel 246050, Belarus

[3]*Department of Chemistry, The University of Alabama*
Tuscaloosa AL 35487-0336, USA

*Corresponding author e-mail: dadixon@ua.edu

Abstract

The irradiation of a poly(vinylidene fluoride) (PVDF) plate with γ-rays up to 100 kGy leads to the breaking of the chain and the formation of unsaturated bonds but practically does not have any effect on the conformation composition of PVDF macromolecules. The main conformer, as in native PVDF, is the β form. Irradiation with an IR laser leads to a noticeable carbonization of PVDF macromolecules and is accompanied by a structural transition of polymer macromolecules from the β conformer to the α conformer. In the IR spectrum of the powdered product from laser ablation of PVDF, in addition to the absorption bands of the ablation crater, absorption bands from the parent PVDF are still present.

Keywords: poly(vinylidene fluoride), γ-irradiation, CO_2 laser ablation, IR spectra.

1.   Introduction

Poly(vinylidene fluoride) (PVDF) is a widely-used polymer with a number of unique physical and chemical properties including mechanical flexibility, high chemical inertness, thermal stability, biocompatibility, lack of "cold flow," and radiation resistance. The polymer dissolves relatively easily in aprotic solvents and is easily processed by pressing, injection molding, and extrusion. It can be welded and painted [1, 2]. Owing to these unique properties, PVDF and other vinylidene fluoride-based polymers rank only below polytetrafluoroethylene in terms of production volume and consumption scale in terms of fluoropolymers [3]. Having high piezoelectric and pyroelectric characteristics, PVDF is the most promising polymer ferroelectric that can be used in a polarized state in different applications [4], including medicine [5]. The use of PVDF as a substrate to create nano- and pico-structures from the carbon (including quasi-one-dimensional structures) on its surface is a promising area of nanotechnology [6]. Of particular interest is production of quasi-one-dimensional carbon from PVDF, first as a model for

the study of the physics of low-dimensional systems, and second because of the prospects for practical applications in microelectronics and nanoelectronics, as well as in optics [7].

There are five types of chain conformations – α, β, γ, α_p, and ε – in semicrystalline PVDF [8, 9]. The most common is α-PVDF with the TGTG conformation form, where T and G are trans and gauche forms of the polymer CH_2–CF_2 groups. The β-PVDF structure responsible for the piezoelectric and pyroelectric properties of PVDF has a flat zigzag conformation TTTT [10, 11]. The γ-structure of PVDF has a TTTGTTTG conformation [12, 13], and the α_p and ε conformations are extremely rare. Currently, there is significant interest in the possibility of increasing the content of the β modification of PVDF, because it can give the polymer high piezo- and pyro-activity [14]. Various approaches have been developed to initiate a structural transition in PVDF to increase the β-form crystallite content, in particular, the method of orientation drawing of PVDF films [15–17] and the introduction of metal particles [18] or nanotubes [19] into the polymer matrix.

$\gamma-$Irradiation doses of up to 500 kGy of the mono- and bi-axially elongated PVDF films [20] lead to an increase in the IR absorption spectral bands of the β-PVDF conformation, consistent with a decrease in the absorption bands due to α-PVDF. The resistance of β-PVDF to irradiation is apparently higher than that for α-PVDF. In addition, polymer powders are also more resistant to irradiation than films prepared from them. A polymorphic transition of the type $\alpha \rightarrow \beta$ was noted [21] on irradiation of PVDF with a dose of $5000 - 6000$ kGy. However, the nature of such structural transitions in PVDF under the action of radiation has not been fully established. The purpose of this work is to use IR spectroscopy to probe PVDF irradiated with γ-rays from a ^{60}Co source and by infrared radiation from a CO_2 laser in vacuum.

2. Experimental

Materials. Commercial Kynar® PVDF was purchased from McMaster–Carr Supply Company (Atlanta, Georgia, USA) and was used as plates of 10 cm thickness.

Laser Irradiation. The process of laser ablation (LA) was carried out in a vacuum chamber system previously described in detail [22]. A CO_2 laser of continuous radiation "LGN-703" with a wavelength of 10.6 μm, power of 40 W, and diameter of the laser beam on the target surface of 9 mm was used. A window made from single crystals of sodium chloride was used to pass the laser beam into the ablation chamber. Before the experiment, the laser was turned on for 5 min to stabilize the laser power and the mode structure of the beam. The LA chamber was evacuated initially up to 1 Pa. The ablation process was also performed with a continuous evacuation of resulting gaseous products of LA.

γ-Irradiation. Preliminary γ-irradiation of the polymers was carried out at a facility (UNU "Gammatok-100" IPCHF RAN) with rays of ^{60}Co source. The dose rate of γ-irradiation was 0.15 Gy/s.

3. Results and Discussion

Native PVDF. A comparative analysis of IR spectra was performed to study changes in the structure of PVDF macromolecules under the influence of IR laser and γ-irradiation. A large number of peaks with the positions of the maxima listed in Table 1 are recorded in the IR spectrum of the original PVDF in the range 600–4000 cm^{-1} (Fig. 1 a). The absorption bands are consistent with known literature data for this polymer. The stereochemical conformations of PVDF can differ both in the number of characteristic

Table 1. The Absorption Bands of the Virgin and Irradiated γ-Rays and IR Laser PVDF Plates.

Dose of γ-irradiation, kGy					Conformation	Assignment[b]
0	50	0	50	0		
IR-laser irradiation time, s						
0	0	20	20	20		
Appearance of the sample						
Plate	Crater of the laser ablation			Powder		
Frequencies,[a] cm^{-1}						
691vw	691vw			691vw	$\gamma-(688)$	$\delta(\mathrm{CF}_2)$ [23]
		763m	763m	763m	$\alpha(763)$ [24]	$\delta(\mathrm{CF}_2)+\delta(\mathrm{CCC})$ [25]
796w	796lb	796m	796m	796m	$\alpha(796)$ [24]	$\tau(\mathrm{CH}_2)$ [23]
841s	841s	841s	841s	841s	$\beta(840)$ [25]	$\tau(\mathrm{CH}_2)-\nu_a(\mathrm{CF}_2)$ [25]
877s	877s	877s	877s	877s	$\beta-(879)$ [25]	$\nu_a(\mathrm{CC})+\nu_s(\mathrm{CF}_2)$ [25]
		975m	975m	975m	$\alpha(975)$ [24]	$\tau(\mathrm{CH}_2)$ [23]
1071s	1071s	1071s	1071s	1071s	$\beta-(1073)$ [25]	$\nu_a(\mathrm{CC})\text{-}\omega(\mathrm{CF}_2)+\omega(\mathrm{CH}_2)$ [25]
1177s	1177s				$\gamma(1176)$ [23]	$\nu_s(\mathrm{CF}_2)+\tau(\mathrm{CH}_2)$ [23]
		1183s	1183s	1183s	$\alpha(1182)$ [25]	$\nu_s(\mathrm{CF}_2)+\tau(\mathrm{CH}_2)$ [25]
		1209lb	1209lb	1209lb	$\alpha(1209)$ [24]	$\nu_a(\mathrm{CF}_2)+\omega(\mathrm{CH}_2)$ [25]
1240w	1240w	1240lb	1240lb	1240lb	$\gamma(1234)$ [24]	$\nu_a(\mathrm{CF}_2)+\omega(\mathrm{CH}_2)$ [23]
1277s	1277s	1277s	1277s	1277m	$\beta(1275)$ [24]	$\nu_s(\mathrm{CF}_2)-\nu_s(\mathrm{CC})+\delta(\mathrm{CCC})$ [25]
		1383lb	1383lb	1383lb	$\alpha(1383)$ [24]	$\delta(\mathrm{CH}_2)+\omega(\mathrm{CH}_2)$ [23]
1401s	1401s	1402s	1402s	1401s	$\beta(1401)$ [25]	$\omega(\mathrm{CH}_2)-\nu_a(\mathrm{CC})$ [25]
1431m	1431m	1431lb	1431lb	1431lb	$\beta(1431)$ [24]	$\delta(\mathrm{CH}_2)-\omega(\mathrm{CH}_2)$ [23]
1453vw	1453wv	1453vw	1453vw	1454vw		$\delta_a(\mathrm{CH}_3)$ [26]
		1599w	1599w	1599w		$\nu(\mathrm{C}{=}\mathrm{C})$ [26]
		1624w	1624w	1624w		$\nu(\mathrm{C}{=}\mathrm{C})$ [26]
	1711vw	1715m	1715m	1715m		$\nu(\text{-CH}{=}\mathrm{CF}_2)$ [27]
	1742w					$\nu(>\mathrm{C}{=}\mathrm{CF}_2)$ [27]
		1753vw	1753w	1754vw		$\nu_s(\mathrm{C}{=}\mathrm{O})$ [28]
2853w	2853w			2855vw	$\beta(2850)$ [29]	$\nu_s(\mathrm{CH}_2)$ [30]
2924m	2924w			2924vw	$(\beta+\alpha)(2890)$ [29]	$\nu_a(\mathrm{CH}_2)$ [30]
				2936vw		$\nu_a(\mathrm{CH}_2)$ [28]
2957vw						$\nu_a(\mathrm{CH}_3)$ [30]
2978lb	2978lb			2978vw	$\beta(2978)$ [23]	$\nu_s(\mathrm{CH}_2)$ [23]
		2986vw		2986vw	$\alpha(2986)$ [23]	$\nu_s(\mathrm{CH}_2)$ [23]
3018vw	3018vw			3018w	$\beta(3020)$ [23]	$\nu_a\ (\mathrm{CH2})$ [31]]
		3024w	3024w	3024w	$\alpha(3026)$ [23]	$\nu_a(\mathrm{CH}_2)$ [31]

[a]Relative intensity, here: s (strong), m (medium), w (weak), vw (very weak), and lb (line bend).

[b]Type of vibration, here: ν_a (antisymmetric stretching vibrations), ν_s (symmetric stretching vibrations), ω ("wagging" vibrations), δ (deformation vibrations), and τ (torsion vibrations). The signs "+" and "−" show the phase relationships.

absorption bands and in their intensity. The types of conformations of macromolecules of the studied samples and the corresponding assignments from the literature are given in Table 1.
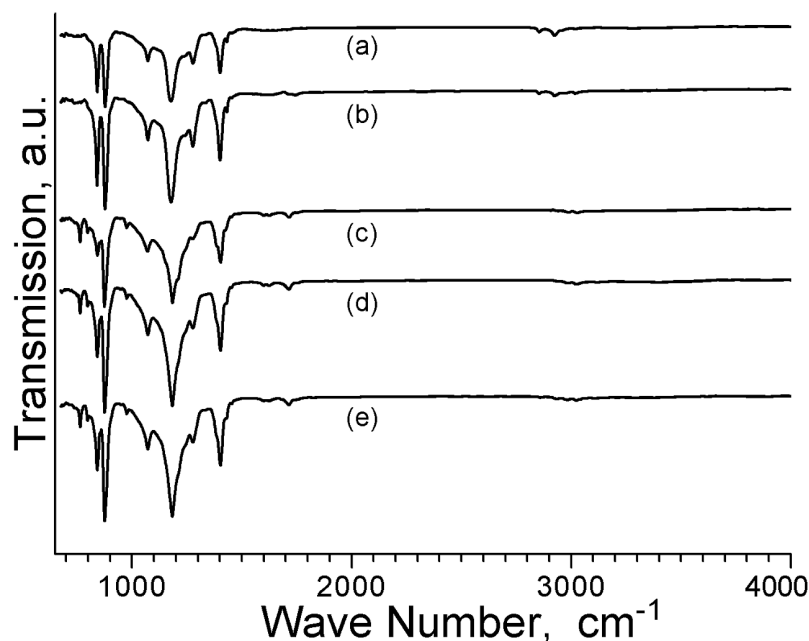

Fig. 1. IR spectra of the virgin PVDF (a) and PVDF irradiated with γ-rays (b, d) and IR laser beams (c, e). Sample (d) is subjected to laser ablation after γ-irradiation; here, dose of γ-irradiation is 100 kGy, and IR irradiation time is 30 s.

The intense absorption bands with peaks at 841, 877, 1071, 1177, 1277, and 1400 cm^{-1} in the mid-frequency region of the IR spectrum are associated with stretching and deformation vibrations of various fragments of the PVDF macromolecule. In the high-frequency region, low-intensity peaks in a wide band in the range from 3050 to 2800 cm^{-1} are due to the asymmetric (2924 and 3018 cm^{-1}) and symmetric (2853 and 2978 cm^{-1}) stretching vibrations of CH_2 groups in the sp^3 valence state, as well as asymmetric stretching vibrations of terminal CH_3 groups (2959 cm^{-1}). The striking differences in the absorption spectra of various conformational modifications of PVDF make it possible to analyze its phase composition. According to the previous work [23], the absorption band of the CH_2 group in the IR spectrum of two-phase PVDF is represented by two peaks, each of which contains the contributions of α (2986 and 3026 cm^{-1}) and β (2978 and 3020 cm^{-1}) conformers. An analysis of the IR spectrum of virgin PVDF (Fig. 1 a) shows that its macromolecules contain only sequentially alternating trans units of the β-phase with characteristic absorption bands at 2.978 and 3.020 cm^{-1}.

γ-Irradiated PVDF. The IR spectrum of γ-irradiated PVDF (Fig. 1 b) is largely identical to the spectrum of the virgin polymer. Some of the differences between them are the reduction in the intensity of the absorption bands at 2924 and 2853 cm^{-1} associated, respectively, with antisymmetric and symmetric stretching vibrations of C–H bonds in the CH_2 group (Fig. 2). This effect is apparently due to the partial carbonization of PVDF macromolecules during radiolysis and decrease in the number of C–H bonds. Another feature of the IR spectrum of γ-irradiated PVDF is the appearance of very weak absorption bands at 1742 and 1711 cm^{-1} (Fig. 2). These bands have been assigned [27] to the $C = C$ stretching vibrations in vinylidene $> C = CF_2$ and vinyl $- CH = CF_2$ groups, respectively. These groups correspond to terminal groups due to breaking of C-C bonds and loss of hydrogen atoms. Thus, the irradiation of the polymer with γ-rays from ^{60}Co with a dose of up to 100 kGy leads to breaking of the chain backbone and the formation of unsaturated bonds but does not affect the composition of PVDF conformers (Table 1).

The main conformer of irradiated PVDF is β-PVDF, as in the origin polymer chain. There is also the possibility of the detachment of hydrogen and fluorine atoms as HF leading to $-\mathrm{HC}=\mathrm{CF}-$ linkages where the polymer backbone is not broken, as observed for X-ray irradiation of PVDF with X-rays generated from a Cu source. This apparently is not an important process here.

IR-Irradiated PVDF. A completely different picture arises in samples treated with IR radiation from a CO_2 laser as the mechanism of the interaction of this wavelength and intensity of light with the polymer is fundamentally different. The energy of a γ-quantum from ^{60}Co (1.2 MeV) can dissociate any intramolecular bond, but the heating of the irradiated sample is relatively low under our conditions. In contrast, the quantum energy of IR radiation is completely insufficient for electronic excitation and cannot lead to dissociation of intramolecular bonds. The interaction of IR radiation with the polymer occurs by the excitation of thermal vibrations.

An intense heating of the irradiation zone leads to the dissociation of chemical bonds (thermal destruction) of the polymer under high-intensity IR radiation, which ensures a sufficiently high density of absorbed power in the polymer. The resulting fragments of macromolecules with various molecular weights evaporate due to ablation of the polymer. At the same time, the macromolecule fragments pass into the ablation flow. Their binding energy with neighboring molecules is less than the strength of intermolecular bonds.

The process of laser ablation of the polymer can be divided into the following stages: (i) the initial period of heating of the surface layer of the polymer target and its melting; (ii) the forcing of the melt from the center of the irradiation zone to the periphery, a process that also occurs in subsequent stages; (iii) the ablation of the degradation products from the macromolecules, which carry along a microdroplet as a low-viscosity melt. As a result of the processes occurring in the second and third stages, a structure is formed with the characteristic shape of a funnel with a melt roller on the periphery (crater of ablation).

Micromelt droplets carried by the intense molecular flow from the crater are deposited on the surfaces surrounding the target in the form of a layer of micropowder. Such a component of the ablation flow is characteristic of many thermoplastic polymers that are not able to cross-link during laser irradiation [32]. Characteristically, the ring around the ablation crater and the melt inside it has a brownish color, the saturation of which increases as the irradiation time increases. This indicates an increase in the number of defects in the laser-modified material as a result of accumulation of molecular chains with double bonds and/or radical centers.

Figures 1 and 2 show the IR spectra of the products of laser exposure to PVDF: the material of the crater formed during ablation of the virgin (spectra labeled as c) and γ-irradiated (spectra labeled as d) polymer, as well as powder deposited on the surface installed in front of the ablative flame (spectra labeled as e). They differ markedly from the IR spectra of the virgin (spectra labeled as a) and γ-irradiated polymer (spectra labeled as b).

In the spectrum of the crater material resulting from the ablation of the virgin PVDF, new absorption bands at 763, 975, 1183, 1209, 1599, 1624, 1715, 1753, 2981, 3024, and 3041 cm^{-1} grow in, and this is accompanied by the disappearance of the absorption bands with frequencies 1177, 1742, 2853, 2924, 2959, 2978, and 3018 cm^{-1}.

The appearance of the absorption bands of the PVDF macromolecule fragments with unsaturated bonds at 1599, 1624, 1715, 1753, and 3041 cm^{-1} indicates a marked dehydrofluorination of the polymer macromolecules. The resulting $\mathrm{C}=\mathrm{C}$ bonds are observed at 1624 cm^{-1}, while the $\mathrm{C}=\mathrm{C}$ conjugated bonds are red-shifted to 1599 cm^{-1}, which is associated with the bathochromic effect. The appearance of the latter in the polymer is accompanied by the appearance of a yellow color up to brown depending
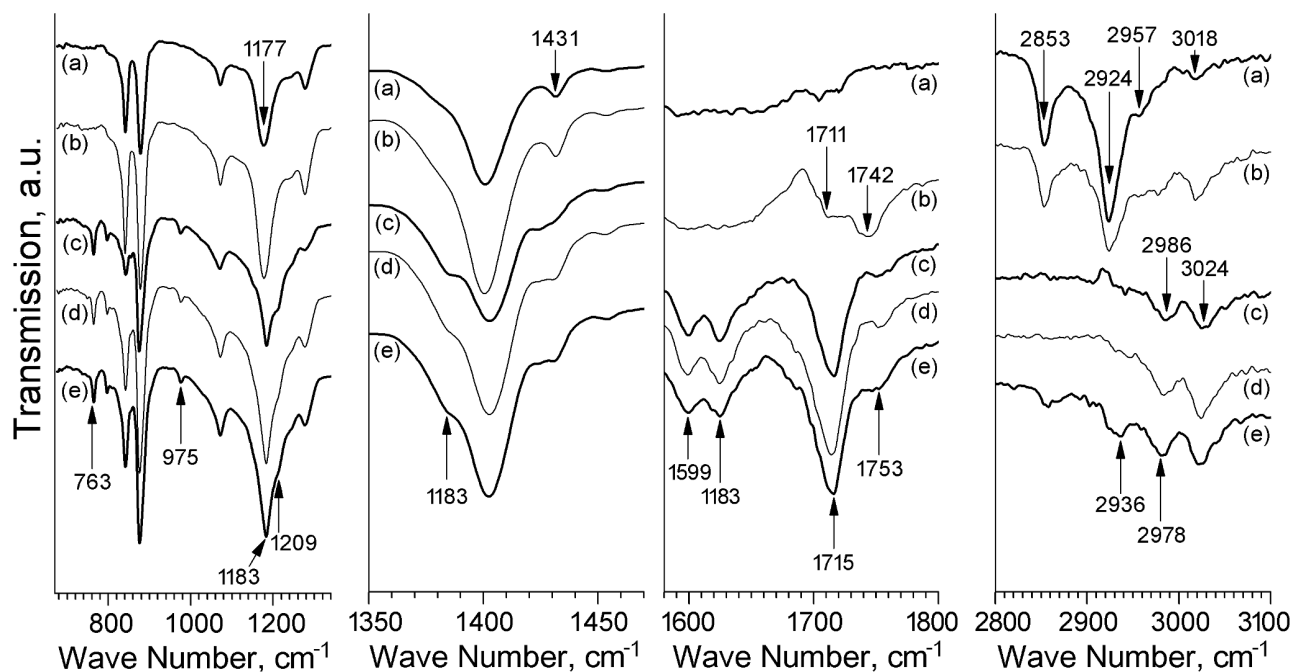
Fig. 2. Expanded IR spectra in different spectral regions of the virgin PVDF (a) and PVDF irradiated with γ-rays (b, d) and IR laser beam (c, e). Sample (d) is subjected to laser ablation after γ-irradiation; here, dose of γ-irradiation is 100 kGy, and IR irradiation time is 30 s.

on the degree of conjugation.

The absorption bands appearing at 763, 975, 1183, 1209, 2986, and 3024 cm^{-1} correspond to the α-conformer of PVDF. The absorption bands at 2853, 2978, and 3018 cm^{-1}, which disappear during the laser ablation, are characteristics of the β-polymer conformer. Consequently, under the action of IR laser beam, there is a structural transition of the polymer from the β- to the α-conformer.

A comparative analysis of the IR spectra of the surface layers of craters formed by laser ablation of the virgin (Figs. 1 c and 2 c) and γ-irradiated PVDF (Figs. 1 d and 2 d) shows that they are similar (Table 1). The difference between the spectra is the presence at 2855 and 2936 cm^{-1}, and the absence at 3041 and 2981 cm^{-1}, of very weak absorption bands in the spectrum of the crater from γ-irradiated PVDF. The largest number of absorption bands are observed in the IR spectrum of the powder formed during laser ablation (Fig. 1 d). In its spectrum, in addition to all the absorption bands in the spectrum of the ablation crater material, are the bands at 691, 2924, 2978, and 3018 cm^{-1}, which are found in the spectrum of the virgin PVDF (Fig. 2 d).

4. Summary

$\gamma-$Irradiation of PVDF under our conditions led to backbone C–C bond cleavage and the formation of shorter polymer chain lengths. This is accompanied by the formation of $C = C$ terminal bonds, but the remaining part of the PVDF has essentially the same conformational properties as that of the virgin polymer, the β-conformation. Significant transformation of the structural–conformational state of PVDF occurs under the action of IR laser radiation in the ablation mode in vacuum. The most modified material

is a micropowder with a low molecular weight formed during ablation and is initially ejected from the crater in the form of microdrops of the polymer melt. The products of IR laser irradiated virgin and γ-irradiated PVDF consist mainly of molecular chains containing α-conformers. In contrast to both types of irradiation noted here, X-ray irradiation can lead to carbonization and the formation of unsaturated bonds as well as polyenyl and alkyl radicals [33]. Thus, different types of irradiation on PVDF lead to very different types of products. Although, the differences can clearly be observed, it is far more difficult to pinpoint the prevalent mechanisms due to differences in the energy fluence, the energy of the individual photons, the irradiation times, and the mode of irradiation in terms of the focal point.

Acknowledgments

References

1. J. C. Salamone (Ed.), *B.-J. Jungnickel Polymeric Materials Encyclopedia*, CRC Press, Boca Raton, FL, USA (1996), Vol. 9, p. 7115.
2. J. Scheirs (Ed.), *Modern Fluoropolymers*, John Wiley, Chichester, UK (1997).
3. [plastpolymer.org/firma.htm accessed February 28, 2019].
4. H. S. Nalwa (Ed.), *Ferroelectric Polymers: Chemistry, Physics, and Applications*, Marcel Dekker, New York (1995).
5. G. Laroche, Y. Marois, R. Guidoin, et al., *J. Biomed. Mater. Res.*, **29**, 1525 (1995).
6. N. A. Mavrinskaya, L. A. Lesin, M. Baumgarten, et al., *Bull. South Ural State Uni. Ser. Math. Phys. Chem.*, No. 7, p. 80. (2008).
7. R. B. Heimann, S. E. Evsyukov, and L. Kavan (Eds.), *Carbyne and Carbynoid Structures*, Kluwer Academic, Dordrecht, Netherlands (1999), p. 333.
8. M. Tazaki, R. Wada, M. Okabe, and T. Homma, *J. Appl. Polym. Sci.*, **65**, 1517 (1997).
9. W. K. Lee and C. S. Ha, *Polymer*, **3**, 7131 (1998).
10. B. Servet, D. Broussoux, F. Micheron, et al., *Rev. Tech. Thomson-CSF*, **12**, 761 (1980).
11. B. Servet and J. Rault, *J. Physique*, **40**, 1145 (1979).
12. A. Salimi and A. Yousefi, *Polym. Test.*, **22**, 699 (2003).
13. T. Bocaccio, A. Bottino, G. Capanelli, and P. Piaggio, *J. Membr. Sci.*, **210**, 315 (2002).
14. A. A. Luschekin, *Polimernie Elektreti (Electric Polymer)*, 2nd ed., Khimiya, Moscow (1984) [in Russian].
15. G. T. Davis, J. E. McKinney, M. G. Broadhurst, and S. C. Roth, *J. Appl. Phys.*, **149**, 4998 (1978).
16. A. Salimi and A. Yousefi, *J. Polym. Sci.*, **42**, 3487 (2004).
17. T. Lei, L. Yu, G. Zheng, et al., *J. Mater. Sci.*, **50**, 4342 (2015).
18. S. Yoon, A. Prabu, K. Kim, and C. Park, *Macromol. Rapid. Commun.*, **29**, 1316 (2008).
19. L. Yu and P. Cebe, *Polymer*, **50**, 2133 (2009).
20. V. V. Kochervinskii, *Vysokomol. Soedin.*, **35A**, 1978 (1993).
21. Ye. L. Gal'perin and B. P. Kosminin, *Polymer Sci. USSR*, **15**, 2895 (1973).
22. E. M. Tolstopyatov, S. R. Allayarov, P. N. Grakovich, et al., *Plast. Massy*, **2012**, No. 6, 13 (2012).
23. V. V. Kochervinsky, *Russ. Chem. Rev.*, **65**, 936 (1996).
24. X. Cai, T. Lei, D. Sund, and L. Linde, *RSC Adv.*, **7**, 15382 (2017).
25. Y. Peng and P. Wu, *Polymer*, **15**, 5295 (2004).

26. D. L. Pavia, G. M. Lampman, G. S. Kriz, and J. R. Vyvyan, *Introduction to Spectroscopy*, 5th ed., Cengage Learning, Independence, KY, USA 2015.
27. E. F. Il'icheva, H. A. Slovokhotova, and I. G. Akhvlediani, *Vysokomol. Soedin.*, **18A**, 209 (1976).
28. A. Kh. Kuptsov and G. N. Zhizhin, *Fourier–Raman and Fourier-IR Spectra of Polymers. A Handbook*, Technosfera, Moscow (2013) [in Russian].
29. G. D. Litovchenko, A. I. Barash, M. P. Zverev, and T. F. Kostina, *Zh. Prikl. Khim.*, **21**, 936 (1974).
30. [5-k.biz/aldegid/spectr/IR/table_1.html accessed March 07, 2019].
31. A. R. Probakaran and S. Mohan, *Asian J. Chem.*, **3**, 232 (1991).
32. E. M. Tolstopyatov, P. N. Grakovich, S. K. Rakhmanov, et al., *Inorg. Mat.: Appl. Res.*, **3**, 425 (2012).
33. Yu. A. Olkhov, S. R. Allyarov, M. Vasiliu, et al., *J. Fluor. Chem.* (June 2019, in press).